Effects of Reinforcement by Both Waste Glass and Barley Straw on Water Resistance, Mechanical, and Thermal Properties of Polyethylene Composite

Nadir Ayrilmis , Anton M. Kuzmin , Kuzmin , Kuzmin Masri, Mohamed Yagoub , Lakhdar Sedira, Petr Pantyukhov , Kuwar Mausam , Kuzmin Mausam , Al-Farraj , Al-Farraj , Al-Farraj , Al-Farraj , Al-Farraj , Mausam , Al-Farraj , A

The water resistance, strength, and thermal properties of the thermoplastic composites were investigated by using different blends of barley stalk flour and waste glass flour as hybrid fillers in HDPE (50 wt%). Virgin E-glass fibers were also used for comparison with the results of the waste glass. The test specimens were prepared by hot-press molding. It was found that the water resistance, tensile strength, and modulus of the HDPE polymer composite prepared with the addition of barley straw flour alone were improved with the use of the waste glass flour and barley straw hybrid. The water absorption (24-h) of the HDPE/barley straw composite was found to be 8.38% while the water absorption decreased to 2.2% in hybrid use with 15 wt% waste glass flour. The addition of the barley straw and waste glass altered the crystalline structure of the HDPE, reducing the melting temperature and melting enthalpy while increasing the crystallinity index. The waste glass provided better thermal stability and a controlled increase in the crystallinity, whereas the glass fiber provided higher crystallinity at the expense of greater disruption to the crystalline structure.

DOI: 10.15376/biores.20.3.5967-5987

Keywords: Glass waste; E-glass fiber; Straw barley; HDPE composite; Hybrid composite; Mechanical properties; Water resistance; Thermal analysis

Contact information: a: Department of Wood Mechanics and Technology, Faculty of Forestry, Istanbul University-Cerrahpasa, Bahcekoy, Sariyer, 34473, Istanbul, Turkey; b: Department of Mechanization of Agricultural Products Processing, National Research Mordovian State University, Saransk 430005, Russia; c: Scientific Laboratory of Advanced Composite Materials and Technologies, Plekhanov Russian University of Economics, Moscow 117997, Russia; d: Laboratoire de Génie Energétique et Matériaux, LGEM, Université de Biskra, B.P. 145, 07000 Biskra, Algeria; e: Hydraulic Development and Environment Laboratory, University of Biskra, B.P. 145, Biskra 07000, Algeria; f: Laboratory of Mechanical Engineering (LGM), University Mohamed Khider of Biskra, B.P. 145, Biskra RP 07000, Algeria; g: Emanuel Institute of Biochemical Physics, Russian Academy of Sciences, Moscow 119334, Russia; h: Higher Engineering School of New Materials and Technologies, Plekhanov Russian University of Economics, Moscow 117997, Russia; i: Department of Mechanical Engineering, GLA University, Mathura, India; j: Department of Mechanical Engineering, PTR College of Engineering and Technology, Thanapandiyan Nagar, Madurai-Tirumangalam Road, Madurai, 625008, Tamilnadu, India; k: School of Automation and Intelligent Manufacturing, Southern University of Science and Technology, Shenzhen 518055, China; l: Department Zoology, College of Science, King Saud University, P.O. Box 2455, Riyadh, Saudi Arabia;

^{*} Corresponding author: sivaresearch948@gmail.com

INTRODUCTION

Economic and environmental impacts are driving research into new materials for construction, packaging, automotive, and other manufacturing applications. One of the most interesting new materials is plant-based, natural fiber-reinforced polymer materials. Thermoplastic composites are widely used in industrial applications in many sectors, particularly automotive and construction. The prices of thermoplastics have generally tended to rise due to fluctuations in fossil fuel supplies. For example, the price of 1 metric ton of high density polyethylene (HDPE) is in the range of 1000 to 1500 USD (Chen *et al.* 2017b; Sumesh and Kanthavel 2022). Due to the high cost of thermoplastics, manufacturers of polymer composites are looking to both develop environmentally friendly products by reducing the thermoplastic content of natural and sustainable raw materials, and to reduce costs by using less petroleum-based thermoplastics. Especially, the use of recycled thermoplastics in biocomposite production is important for the effective use of thermoplastics in countries where petroleum-based polymers are insufficient.

The use of agricultural wastes generated during the harvesting in the agricultural sector for producing a variety of value-added products has attracted the attention of both scientists and industrial producers due to their significant advantages. The most important of these advantages are low carbon footprint, renewable raw material, low density, low price, and harmlessness to human health during processing operations (Nur Diyana et al. 2022; Gurupranes et al. 2023). The use of agricultural wastes to improve the mechanical properties of petroleum-derived thermoplastic matrices and reduce their negative impact on the environment is an important potential. Barley (Hordeum vulgare) is one of the most important grain crops in the world today, ranking fourth in terms of both production and cultivated area. In general, the production of 1.0 kg of barley produces 1.2 kg of barley straw as a by-product, which is usually used for fuel and energy production (Kim and Dale 2004). Previous studies have reported that barley straw can be successfully used as a filler in thermoplastic composites (Puglia et al. 2020; Serra-Parareda et al. 2020; Sumesh et al. 2022; Kuzmin et al. 2021, 2024). These studies reported that the addition of barley straw to the thermoplastic composite improved the mechanical properties, but the water behaviour was poor due to its hydrophobic structure.

Among the silicate and aluminosilicate finishing materials, glass deserves special attention. Glass represents a significant proportion of the total solid waste generated worldwide each year. In general, glass is a chemically very stable material that can be reused indefinitely without degradation of its molecular structure (Sanjay and Yogesha 2017; Zafar et al. 2024; Ramakrishnan et al. 2025). As a result, the management and collection of waste glass is becoming an increasingly important part of environmental planning in developed regions. According to the latest data, over 13.5 million tonnes of glass containers are recycled in Europe each year. This represents a recycling rate of over 78% (Pahlevani and Sahajwalla 2018; Arivendan et al. 2024). It is important to investigate added value applications in the recycling of glass, which plays an important role in our lives today, particularly in sectors such as packaging and construction. However, it is generally considered technically very difficult and uneconomical to separate bulk waste glass into different types of glass and to remove contaminants. The diversion of glass into natural fiber composites can provide a low-cost feedstock for manufacturing while addressing a new challenge of bulk waste. A previous study reported that glass fiber can be used in wood plastic composites (WPCs) (Sanjay and Yogesha 2017). They reported that the glass-reinforced WPC had higher modulus of elasticity (MOE), with an increase of about 0.5 GPa per 5 wt% addition of glass flour. The resulting composite was less porous and had better water resistance. In another study, Chen *et al.* (2017a) investigated the effect of hybrid use of the recycled fiber and corn straw fiber in WPCs. They found that the change in the bending and tensile strengths of WPC containing waste glass increased by 23% and 31%, respectively, compared to WPC.

There is a gap in this field due to the lack of sufficient studies on the use of waste glass in natural fiber composites, although virgin glass fibers has been investigated. In particular, the lack of studies on the hybrid use of waste glass and agricultural wastes in polymer composites will be useful to better understand the synergistic effect of these two potential wastes. Although the use of barley stalk as a filler in the production of thermoplastic composites has been considered in previous studies, the effect of its use with waste glass on the polymer composite has not yet been investigated. As a comparison, virgin E-glass fiber was also mixed with barley stalk and used as filler in the polymer matrix. Previous studies reported that barley straw, being a lignocellulosic raw material, had a water absorbing property (Puglia et al. 2020; Kuzmin et al. 2021; Anjumol et al. 2023), which negatively affects the dimensional stability of the polymer composites. Glass is a non-porous and amorphous material with a low water absorption (Pahlevani and Sahajwalla 2018; Karthik et al. 2024; Aruchamy et al. 2025). In order to minimize negative characteristics, such as lower water resisance, the idea of hybridiation of barley straw with hydrophic filler, which is waste glass, was the motivating factor to initiate this study. The water resistance, strength, and thermal properties of the composite were investigated by using different blends of barley stalk (35 to 45 wt%) and waste glass (5 to 15 wt%), which have an important place in the world, as hybrid fillers in HDPE (50 wt%) composite. Virgin E-glass glass fibers were also used for comparison with waste glass.

EXPERIMENTAL

Materials

High density polyethylene (code: HDPE 273-83) produced by Kazanorgsintez PJSC company, Kazan city, Russia) was used as the polymer matrix. The density and melt flow index of the polymer used were 0.95 to 0.96 g/cm³ and 0.40 to 0.65 g/10 min, respectively. The tensile strength and elongation at break of the HDPE were 22.6 MPa and 700%, respectively.

The barley straw was collected from an agricultural field in the Lchalkovsky district of the Mordovia region of the Russian Federation. First, the barley straw was chipped using a chipper. The chips were then ground in a rotary knife mill (model: Retsch PM 120, Germany). The particle size of less than 250 microns was used as a natural filler (Fig. 1).

Waste glass in the form of bottles was randomly collected, washed with warm water, dried, and crushed in a rotary knife mill. A fraction of less than 100 microns was then selected by sieving for further grinding in a planetary ball mill. A Fritsch Pulverisette 7 planetary ball mill (Idar-Oberstein, Germany) was used for fine grinding. The crushed waste glass flour was poured into a jar containing steel balls. The drum rotated at 800 rpm for 15 minutes. After the planetary ball mill, the particle size of the waste glass flour was less than 20 microns (Fig. 2). No surface treatment was applied to the virgin glass fiber, waste glass flour, or to the BSF.

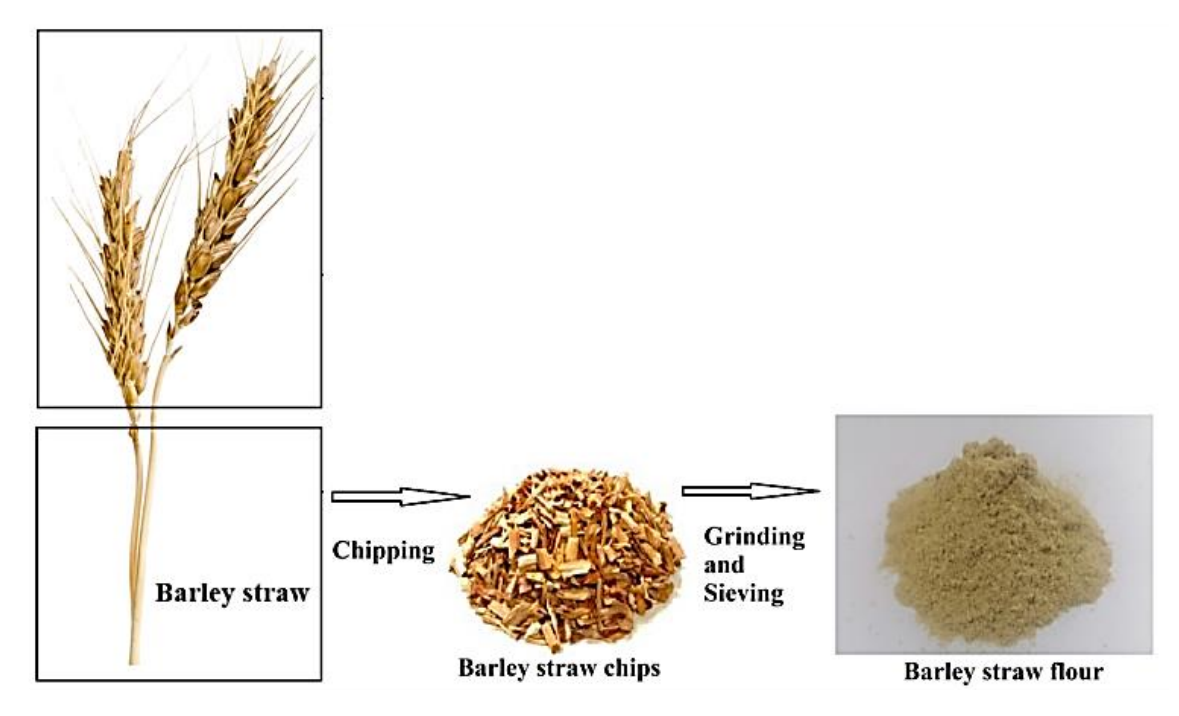


Fig. 1. Barley straw flour (BSF)



Fig. 2. Preparation of the waste glass flour

The virgin E-glass fibers were supplied by Graphite Pro Company in Moscow, Russia (Fig. 3). The length and diameter of the E-glass fibers were 200 microns and 9 microns, respectively. Their specific gravity was $2.50 \, \mathrm{g/cm^3}$ and the softening temperature was approximately 840 °C.

Fabrication of the Composites

Compounding of the polymer matrix and fillers was carried out on a laboratory rotary batch mixer with roller rotors (model: Hakke Rheomix 600 OS, Thermo Fisher Scientific Inc, Massachusetts, United States). The mixing temperature was 150 °C, the rotor speed was 50 rpm, and the mixing time was 15 minutes. First, the polymer was poured into the mixer and then melted. Then the BSF and glass fiber or waste glass were added (Puglia *et al.* 2020). The resulting mixture was compressed on a Gibitre hydraulic press (Gibitre Instruments Company, Bergamo, Italy) at a temperature of 150 °C and a pressure

of 3 MPa (Fig. 4). The thickness of the specimens was 1.25 mm. The tensile specimens with a size of 200×200 mm in the form of a dog bone were punched out from the composite panels. The mean densities of the composites ranged from 1070 to 1197 g/cm³. The experimental design is given in Table 1.



Fig. 3. E-glass fibers



Fig. 4. The composite specimens produced

Specimen	HDPE	Waste Glass Flour	Virgin	Barley Straw Flour
Code	(wt%)	(wt%)	E-Glass Fiber	(wt%)
			(wt%)	
A5	50	5	-	45
A10	50	10	-	40
A15	50	15	-	35
B5	50	-	5	45
B10	50	-	10	40
B15	50	-	15	35
HDPE/BSF	50	-	-	50
HDPE	100	-	-	=

Table 1. The Raw Material Composition of the Composites Produced

Characterization

Water absorption and tensile properties

Tensile strength and modulus tests were performed on a universal testing machine (model: Gotech UAI-7000 M, Gotech Testing Machines Inc., Taiwan) at a temperature of 23±1 °C. The speed of movement of the clamps was 1.0 mm/min. The density of the composites was determined on an H-200L density meter with an ultra-high resolution of 0.001 g/cm³. The tensile and flexural properties of the composites were determined according to ISO 527-2:2012 and ISO 178:2010, respectively. The water absorption test of the composites was performed according to ISO-62:2008 standard. The water moisture absorption of samples with a size of 3 cm × 3 cm was determined by immersion in normal water for 400-h. Five specimens were used for each type of test. All the specimens were conditined in a climate chamber at 20 °C and 50% relative humidity according to ISO 291:2008 before the tests.

Water Absorption Modelling

Diffusion theory was employed to understand the mechanisms involved in the process of water absorption within the composites. Diffusion is defined as the process by which matter is transported from one point within a system to another, as a consequence of random molecular motions (Prasad *et al.* 2023). The fitting of water absorption curves to Fick's model is a common approach for determining the diffusion coefficient (*D*) in composite materials. Water absorption in these materials follows Fickian diffusion behavior, where moisture uptake increases over time and eventually reaches equilibrium. The mathematical model was derived from Fick's second law in one dimension,

$$\frac{\partial C}{\partial t} = D \frac{\partial^2 C}{\partial^2 x} \tag{1}$$

where C is the moisture concentration (%), t is time (h), x is the position, and D is the diffusion coefficient. For thin composites, the water absorption is often expressed as,

$$M_{t} = M_{\infty} \left(1 - \frac{8}{\pi^{2}} \sum_{n=0}^{\infty} \frac{1}{(2.n+1)^{2}} e^{\frac{-(2.n+1)^{2} \pi^{2} D}{h^{2}} t} \right)$$
(2)

where M_t is the mass of absorbed water (g) at time t (h), M_{∞} is the equilibrium water absorption (%), and h is the thickness (mm) of the composites.

To compute *D*, an iterative optimization technique (Orthogonal Distance Regression Algorithm) was applied by minimizing the square error between the experimental water absorption data and the theoretical Fickian model.

Thermogravimetric (TG) Analysis

The TG analysis was conducted using the Perkin Elmer Diamond TGA/DTGA equipment (Perkin Elmer, Waltham, MA, USA) under N_2 atmosphere. The temperature ranged from 30 to 600 °C, with a heating rate set at 10 °C/min.

Differential Scanning Calorimetry (DSC) Analysis

The DSC analysis was carried out using a Perkin-Elmer Diamond DSC equipment under N_2 atmosphere. This method makes it possible to determine the melting and crystallization temperatures as well as the enthalpies of the reaction. A heating/cooling/heating cycle was performed for the thermal characterization of the composites (Gopinath *et al.* 2021). The measured samples were heated from room temperature to 200 °C at a heating rate of 10 °C/min. The crystallinity index (X_c) of the HDPE component was calculated using the enthalpies obtained by integrating the melting peaks of the composites from the DSC analyses. The calculation was adjusted to account for the proportion of the BSF in the composites not undergoing melting compared to the polymer. The value considered for the enthalpy of 100% HDPE is 293 J/g (Awal *et al.* 2010). The crystallinity index values in the composites were obtained according to the formula presented in Eq. 3,

$$X_c(\%) = \frac{\Delta H_m}{\Delta H_{100\%}} \times \frac{100}{w} \tag{3}$$

where ΔH_m is enthalpy of fusion calculated in the composite, $\Delta H_{100\%}$ denotes the enthalpy of fusion of neat HDPE, and w is fraction of the HDPE polymer matrix in the blend.

RESULTS AND DISCUSSION

Water Absorption Behavior with Fick's Diffusion Theory

The water absorption trends of the HDPE/BSF composites with virgin glass waste flour or glass fiber are presented in Figs. 5 and 6, respectively. As expected, the highest water absorption was found in the HDPE/BSF composites, followed by the filled with glass fiber and waste glass, respectively. The increasing addition of the glass fiber in the HDPE/BSF composites decreased the water absorption of the composites. A considerable decrease in the water absorption of the HDPE/BSF composites was found with increasing glass content. The decrease in the water absorption due to the replacement of the BSF flour with the glass fibers or waste glass in the HDPE polymer can also be explained by the nonhygroscopic nature of the glass. The 24-h water absorption of the HDPE/BSF of the composites was 8.41%. When the amounts of the waste glass in the WPC were 5 wt%, 10 wt%, and 15 wt% in the HDPE/BSF composite, the 24-h water absorption values were found to be 5.4%, 4.0%, and 2.2%. At the same loading levels of the glass fiber, the 24-h water absorption values were 3.41%, 2.93%, and 2.19%. When the soaking time was extended to 400-h, the water absorption values of the HDPE/BSF composites with the waste glass at the loading levels of 5 wt%, 10 wt%, and 15 wt% were 11.51%, 10.09%, and 8.38%, respectively. The water absorption of the HDPE/BSF composites with the glass fiber at the same loading levels was found to be 11.48%, 8.49%, and 7.61%, respectively.

These results showed that glass fiber was more effective relative to the water absorption of the composites in the short immersion while the waste glass was more effective in the prolonged immersion.

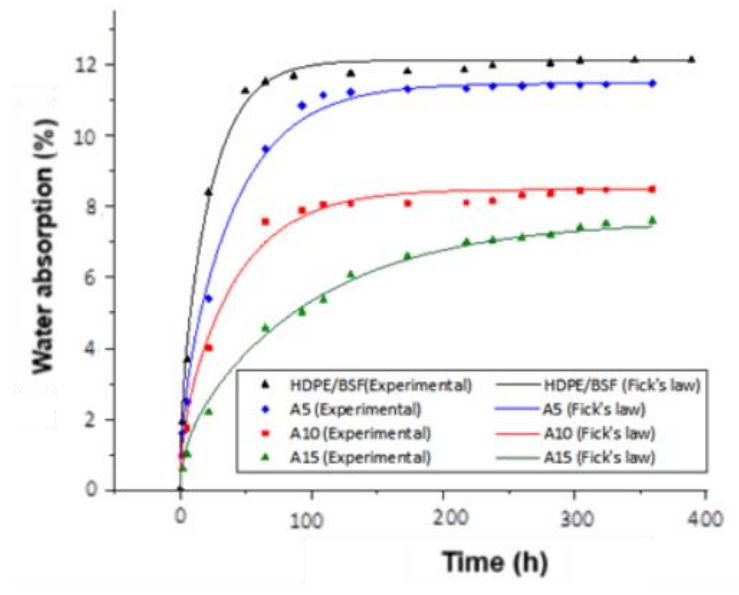


Fig. 5. Experimental and diffusion curves (Fick's law) of water absorption behavior of the waste glass flour/barley straw reinforced composites

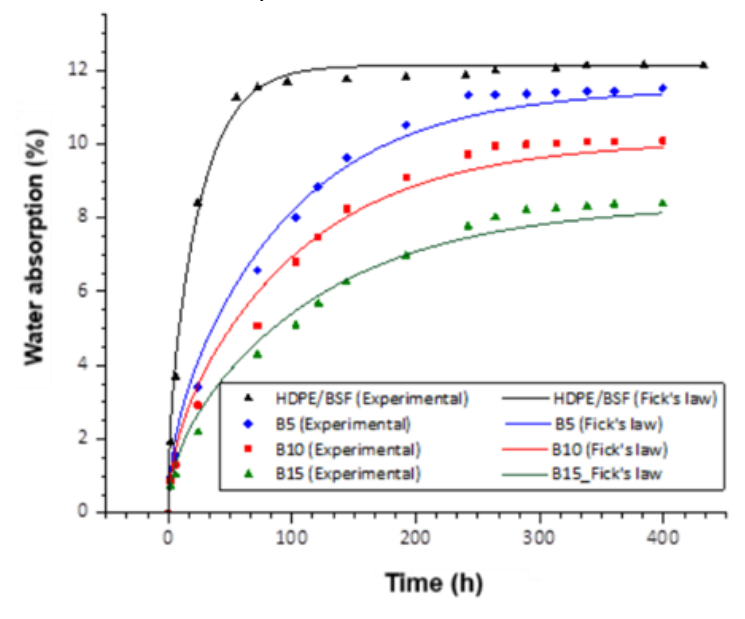


Fig. 6. Experimental and diffusion curves (Fick's law) of water absorption behavior of the virgin glass fiber/barley reinforced composites

When glass fiber was added to the HDPE/BSF at 5 wt%, 10 wt%, and 15 wt% loadings, the water absorption values were lower than those produced by adding waste glass in short-term (24-h) water immersion, but the opposite results were obtained in long-term water soaking (400-h).

When glass fiber and waste glass flour were added in the HDPE/BSF composite at the loading level of 5 wt%, the water absorption was considerably lower than the

HDPE/BSF because of short-term soaking in water, while this difference decreased as a result of long-term soaking. When the immersion time of the HDPE/BSF composite without glass particles was increased from 24-h to 400-h, the water absorption increased from 8.4% to 12.1%. Therefore, the water absorption of the composite because of prolonged soaking was not considerably affected by the addition of 5 wt% glass fiber or waste glass. However, a notable significant decrease in the water absorption rate was detected when the ratio increased to 15 wt%. It is noteworthy that the HDPE composites with higher waste glass content reached equilibrium faster and at lower absorption levels (Fig. 5). A similar result was observed in the composites containing virgin glass fibers (Fig. 6). The long immersion time of the specimens (400-h) provides valuable information on the long-term water absorption behaviour of these composites. Based on the significant reduction observed in water uptake due to the increased waste glass content, the composites with higher glass content retain their physical integrity and appearance more than those with less or no glass content (Sathish *et al.* 2017; Prasad *et al.* 2023).

The reason for the lower water absorption of the HDPE/BSF composites with glass fiber can be explained by the fact that better distribution of the glass fibers in the polymer matrix. Higher amount of the filler led to agglomeration after approximately 55-h of soaking in water, a generally stable trend was observed in the water absorption, while this situation was detected after 250-h in composites with glass fiber additives and after 150-h in composites containing glass flour (except 15%). The decrease in the water absorption of HDPE/BSF composites with glass fiber or filler additives can be explained by their hydrophobic structure. However, as seen in Figs. 5 and 6, the decrease in the difference between the water absorption and the water uptake rate of HDPE/BSF composites as a result of prolonged soaking in water due to increasing filler ratio can be explained by the agglomeration problem and the increase in the number of microvoids (Ashori and Nourbakhsh 2008; Then et al. 2013; Tan et al. 2017; Ramakrishnan et al. 2024). In addition, with prolonged exposure to water, the hydrophobic structure of the BSF powder will absorb water, resulting in microcracking and incompatibility between the waste glass powder and the BSF, as well as between the BSF and the HDPE matrix. Similar results were found in previous natural and synthetic fiber hybrid polymer composites (TabkhPaz et al. 2013; Mayandi et al. 2020; Kar et al. 2024; Kuzmin et al. 2024).

The diffusion coefficient (D) was determined using Fick's second law, optimized via iterative least squares fitting. The trends observed in Figs. 5 and 6 of diffusion behavior are consistent with the water absorption data. It is noteworthy that the water absorption curves followed Fickian diffusion, characterized by an initial linear region (slope) proportional to square root of time and an asymptotic plateau (equilibrium moisture content). The slope of the absorption curve was influenced by the barley straw content: higher barley straw flour increased water absorption due to its hydrophilic nature. In contrast, glass fiber and waste glass flour contents reduced the slope by acting as moisture barriers. However, both glass fiber and waste glass flour showed almost the same slope for 15% (5.24 $\times 10^{-7}$ mm²/s and 5.69 $\times 10^{-7}$ mm²/s, respectively), whereas for small weight fractions, the glass fiber showed lower initial absorption rates than waste glass flour due to its smoother surface and lower porosity. This was also confirmed by the inferiority of its diffusion coefficients given in Table 2. As regards the equilibrium regime, higher barley straw content (50 wt%) showed the higher equilibrium moisture (12.13%) and therefore, the higher amount of the waste glass flour or glass fiber reduced the final moisture absorption. It should be noted that glass fiber provided slightly better resistance to moisture uptake than waste glass flour. Diffusion theory revealed the relationship between fiber

loading and filler hybridization, as well as apparent diffusion coefficients in composites. Based on the results obtained, it can be concluded that the composites with higher glass fiber or waste glass flour content (15%) offered better moisture resistance, making them suitable for applications requiring durability in humid conditions.

 Table 2. Diffusion Coefficients of the Specimens based on Fick's Second Law

Specimen Code	Diffusion Coefficient (mm ² /s)	Standard Error
HDPE/BSF	2.4013E-06	1.1286E-07
A5	1.3543E-06	5.5609E-08
A10	1.3431E-06	8.4561E-08
A15	5.6890E-07	1.5281E-08
B5	6.5253E-07	2.8537E-08
B10	6.0450E-07	3.1573E-08
B15	5.2408E-07	2.4713E-08

Tensile Properties

The results for the mechanical properties are given in Table 3. The tensile strength of the neat HDPE was the 22.6 MPa. The main reason for the significant decrease in the tensile strength of HDPE with the addition 50 wt% filler (the BSF fiber and glass fiber or flour) is the insufficient interfacial adhesion between the polymer and filler. A similar result was observed for the virgin glass fibers. Among the composites, the highest flexural strength and flexural modulus were found in the HDPE composites filled with the BSF/glass waste flour, followed by the BSF/virgin glass fibers, and the BSF fibers, respectively. The addition of the virgin glass fiber or waste glass flour to the HDPE/BSF composite improved the tensile strength and modulus. The tensile strength and modulus of the HDPE/BSF composites were found to be 11.2 MPa and 1662 MPa, respectively. The tensile strength and modulus increased to 15.8 MPa and 1740 MPa, respectively, when the 15 wt% waste glass flour was added into the HDPE/BSF composite. A similar result was found for the glass fibers (Table 3).

Table 3. The Mechanical Properties of the HDPE/BSF Composites with Virgin Glass Fiber and Waste Glass Flour

Composite Type*	BSF (wt%)	Waste Glass wt%)	Virgin E- Glass Fiber (wt%)	Tensile Strength (MPa)	Tensile Modulus (MPa)	Elongation at Break (%)
A5	45	5	-	14.3 (0.9)	1680 (95)	5.5 (0.2)
A10	40	10		15.5 (1.1)	1695 (185)	6.1 (0.4)
A15	35	15		15.8 (1.3)	1740 (130)	6.3 (0.3)
B5	45	-	5	14.1 (0.6)	1691 (65)	4.3 (0.1)
B10	40	-	10	14.8 (1.2)	1684 (160)	4.3 (0.3)
B15	35	-	15	15.1 (1.3)	1625 (150)	4.1 (0.3)
HDPE/BSF*	50			11.2 (2.0)	1662 (165)	5.0 (0.3)
HDPE***	100	-	-	22.6	-	700

^{*}All the composites contain 50 wt% HDPE matrix. ** The values from the data sheet of the supplier. The values in the paranthesis are the standard deviations.

The HDPE composites with a hybrid of the waste glass and the BSF had higher tensile strength and modulus than those of the HDPE composites filled with the BSF alone.

This could be explained by the higher modulus of elasticity of glass waste (Bambach 2020; Sumesh et al. 2024). Another interesting result was that the strength properties of HDPE/BSF composites containing waste glass flour were higher than the HDPE/BSF composites containing virgin glass fiber. This can be explained by the higher aspect ratio of the glass fiber compared to the waste glass flour. The higher aspect ratio enhances stress transfer from the matrix to the fiber, hereby improve the tensile properties (Zhang et al. 2020). The average length (15.8 micron) of the waste glass particles was longer than that (15.1 micron) of the waste glass fibers. In general, there was not much increase in the tensile strength and modulus of the composites when the addition of waste glass flour increased from 10% to 15%. A similar situation was found for composites produced by adding virgin glass fibers. This can be explained by the agglomeration of the filler in the polymer (Chen et al. 2017). Especially, when the amount of the glass fiber reached to 15 wt% in the composite, it may cause agglomeration, which adversely affects the stress transfer and as a result, the tensile modulus decreases (Ayrilmis et al. 2024) When the 50 wt% BSF flour were added to the HDPE matrix, the elongation at break value showed a definite decrease from 700 to 5%. The elongation at break decreased with increasing glass fiber or waste glass flour content in HDPE/BSF composite.

TG Analysis

The TG curves of the thermal decomposition of HDPE/BSF/glass composites are presented in Fig. 7. For the neat HDPE, one can distinguish three stages. In the first range 80 to 386 °C, a small weight loss with a slight downward slope was observed. A mass lost equal to 2.13% was measured and can be attributed to the evaporation of low molecular weight components, such as unreacted monomers, additives, or moisture released to the environment. The second stage represented the main part of the pyrolysis process, this step occured around 386 to 510 °C and remained as the temperature increased (Suja *et al.* 2024).

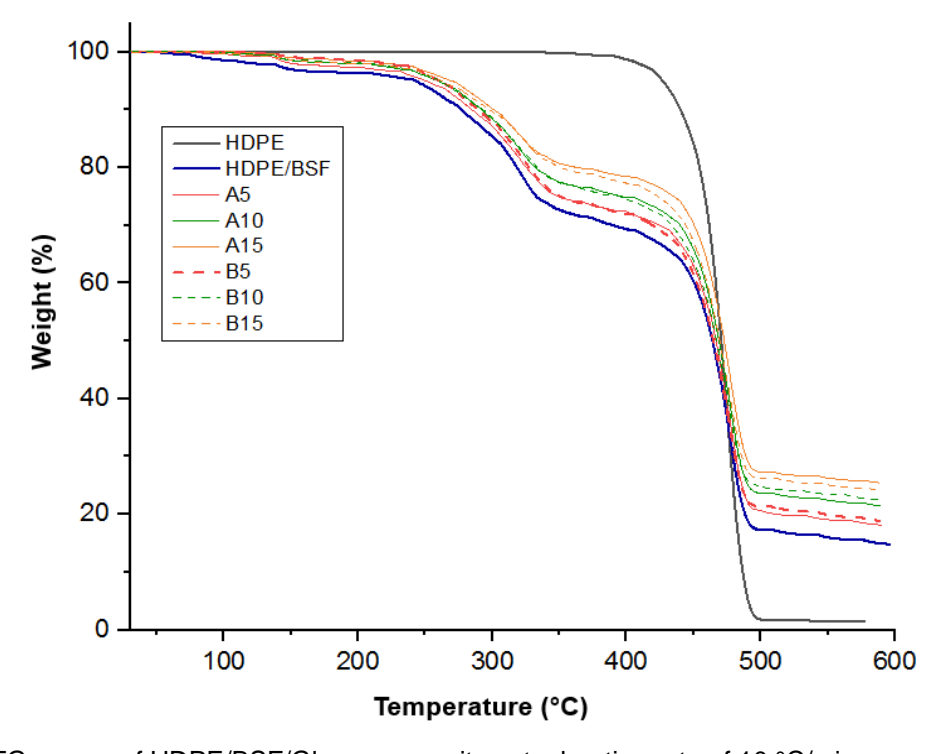


Fig. 7. TG curves of HDPE/BSF/Glass composites at a heating rate of 10 °C/min

The TG curves of the HDPE/BSF glass-reinforced composites are depicted in curves (A5, A10, A15) and (B5, B10, B15) for the glass fiber and waste glass reinforcement (5%, 10%, and 15%), respectively (Fig. 7). In lower temperatures (up to about 140 °C), an initial weight loss that was able to reach 1.35%. This was somewhat less than for the HDPE/BSF processed alone (2.42%). This is due to the evaporation of moisture from the BSF, unlike the waste glass and fibers that typically show almost no loss in this temperature interval. Above 140 °C, the degradation rate decreased; nevertheless, the loss of weight continued, and these remained proportional to the quantity of glasses added. Thereafter, a significant weight loss was observed in the range of 240 to 330 °C. The degradation accelerated to reach a maximum rate of (2.51% to 3.19%/min) and a weight loss between (13.47% to 18.2%) at 316 to 324 °C.

As the temperature was further increased, degradation occurred between 360 °C and 440 °C. This was confirmed by the HDPE/BSF curve (Fig. 7). It was characterized by a small downward slope of mass loss, which may be related to the gradual decomposition of the cellulose and lignin. At higher temperatures, typically around 475 °C (second peak), the HDPE/BSF composite showed a higher rate of mass loss (13.69 %/min), with only 35.3% of the weight remaining. This may be related to the thermal behaviour of pure HDPE, where its fast degradation occurred at almost the same temperature (Fig. 8 and Table 4). The degradation process then slowed down and converged to zero velocity. A major degradation stage was observed at the end of the thermal treatment, reaching 85.2% of the initial mass.

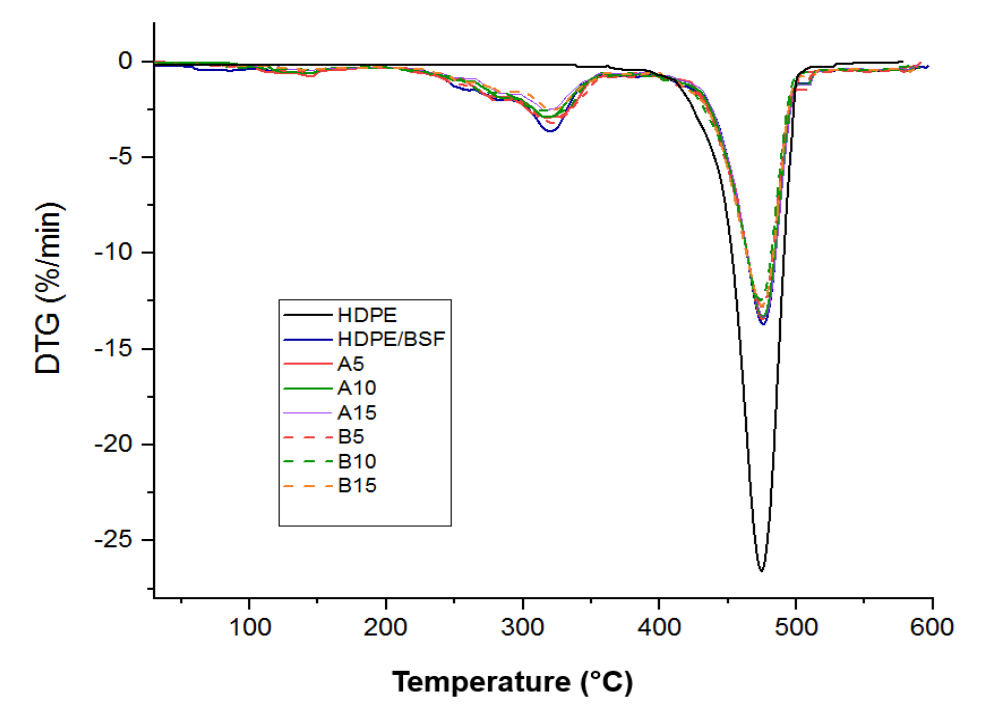


Fig. 8. First derivative TG curves (DTG) of the HDPE/BSF/Glass composites at a heating rate of 10 °C/min

At lower temperatures, typically below 230 °C, the TG curve showed an initial weight loss due to evaporation of moisture and VOCs from both the HDPE matrix and the BSF. This region appeared as the first slight slope on the TG curve and has been confirmed by several researchers, including Palumbo *et al.* (2015). As the temperature was increased,

a second significant loss in mass occurred between 230 and 320 °C with a linear decrease in the mass loss. It reached a maximum velocity (3.62 %/min) at 319 °C (first peak). This decomposition was mainly attributed to the breakdown of the hemicellulose, which was one of the primary constituents of the BSF. The degradation of the hemicelluloses could release volatile gases such as acetic acid, furfural, and other smaller molecules. At high temperatures, some low molecular weight components could also be expected to be released from HDPE through polymer chain cleavage. In the middle temperature range of the TG curve, *i.e.*, 320 to 360 °C, a further mass loss of approximately 7.65% was observed.

Table 4.	TG/DTG	in Critical	Regions
----------	--------	-------------	---------

Parameter		HDPE	HDPE /BSF	Specimen Code					
		TIDI L		A5	A10	A15	B5	B10	B15
	Temperature (°C)	-	319.6	318.1	317.9	316.42	321.1	324.8	319.1
First	Weight TG (%)	-	79.6	82.2	84.2	86.53	81.8	82.5	85.8
peak	DTG (%/min)	-	3.62	2.90	2.89	2.52	3.19	2.70	2.51
Second peak	Temperature (°C)	474.8	475.9	475.4	475.6	476.4	475.1	473.9	474.8
	Weight TG (%)	38.2	35.3	38.6	41.2	44.9	37.7	41.95	43.5
	DTG (%/min)	26.6	13.69	13.4	13.3	13.3	12.8	12.4	12.7
Final weight	Temperature (°C)	591.1	596.4	597.5	589.6	588.7	588.3	588.6	589.1
	Weight TG (%)	1.69	14.8	18.4	21.5	24.5	18.9	22.6	24.1
	DTG (%/min)	0.02	0.219	0.05	0.31	0.16	0.25	0.06	0.29

The weight loss may be related to the decomposition of hemicelluloses, cellulose, and partial degradation of the lignin from the BSF, as with the TG behaviour of the HDPE/BSF composites. Weight loss was typically close to the amount of HDPE and proportional to the weight of fiberglass or waste glass. Once again, these degradations were less than occurred for the HDPE/BSF composite, where an amount of 20.4% was noticed in Table 4. At medium temperatures (330 to 360 °C) the rate of mass loss decreased slightly and tended to zero. This may be due to the thermal resistance of the lignin, HDPE, and mineral components. Subsequently (between 360 and 475 °C), the weight of the composites showed a steep downward slope. All the DTG curves for the glass-based composites showed the same maximum degradation rates with an average of 13%/min. This value was slightly lower than HDPE/BSF and remained lower than pure HDPE. However, all the composites reached their peak at the same temperature, indicating that both HDPE and lignocellulosic organic fillers were completely degraded at this temperature (Ayrilmis et al. 2024). For the ultimate temperature, glass-reinforced composites showed the largest amounts of dry residue (Fig. 9). These amounts were not affected by the type of glass and were found to be proportional to the weight fraction of glass added, whether virgin glass fiber or waste glass flour. On the other hand, the solid remaining in HDPE/BSF also showed significant charred residues. The final weight losses of the composites are shown in Fig. 9.

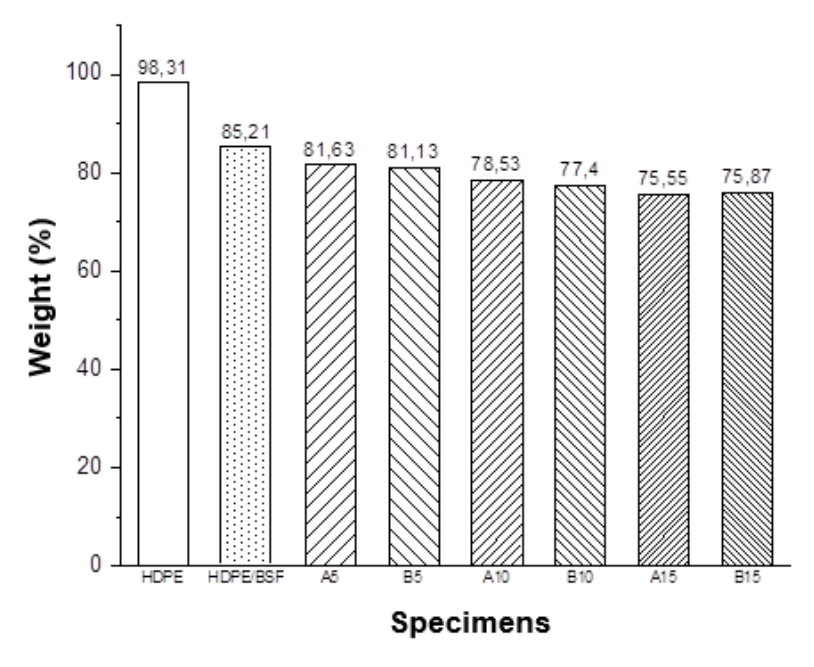


Fig. 9. Final weight loss of composite materials

The highest rate of mass loss of (26.6 %/min) was achieved at 474.8 °C, which corresponded to 38.2% of the HDPE residue left. From the literature, a close range of degradation (360 to 550 °C) was found by Jeziorska *et al.* (2017). Above 544 °C up to 600 °C, the TG curve showed a final degradation of HDPE with a net weight loss equal to 98.3%. Similar findings were reported by Saleh *et al.* (2020), where an amount of 95% of HDPE degradation occurred at 498 °C and increased to 99.99 % of residue left at 592 °C. All the mass loss was linked to the BSF and more particularly to the decomposition process of cellulose, the major component of the BSF. The cleavage of cellulose chains into smaller fragments such as levoglucosan ultimately resulted in the charred residues; the decomposed BSF was almost equal to 61.5% of its initial mass. Chen *et al.* (2011) found similar results in the study of the degradation of untreated and treated straw flours. It should be noted that the HDPE thermal degradation is mainly due to the random scission of polymer chains, resulting in the release of ethylene, small amounts of methane, and charred residues. The results showed that the interaction between the HDPE and the BSF influenced the thermal degradation and possibly modified the thermal degradation pathway.

DSC Analysis

The DSC curves showing the differential thermal analysis of HDPE and HDPE/BSF composites, as well as glass fibers or waste glass used as modifiers, are provided in Fig. 10. The onset temperature ($T_{\rm m}$ onset), end temperature ($T_{\rm m}$ end set), melting temperature ($T_{\rm m}$), enthalpy of fusion ($\Delta H_{\rm m}$), and degree of crystallization ($X_{\rm c}$) of the composites were determined. The results of the DSC analysis are summarized in Table 5. The analysis of $T_{\rm m}$ showed that the neat HDPE had the highest melting temperature at 140.0 °C, indicating a well-ordered crystalline structure. Makhlouf *et al.* (2022) also found a melting peak at 144 °C. The addition of the BSF to the HDPE slightly reduced this temperature to 135.6 °C, suggesting a disruption of the HDPE crystalline matrix. The composites with waste glass exhibited melting temperatures that decreased with increasing waste glass content (A5 = 135.5 °C, A10 = 133.2 °C, A15 = 134.5 °C), indicating increased

disruption of the HDPE crystallinity. Similarly, the composites with the glass fiber showed lower melting temperatures than the neat HDPE (B5 = 132.5 °C, B10 = 133.6 °C, B15 = 134.4 °C). Similar findings were also observed in a previous study (Chen *et al.* 2011).

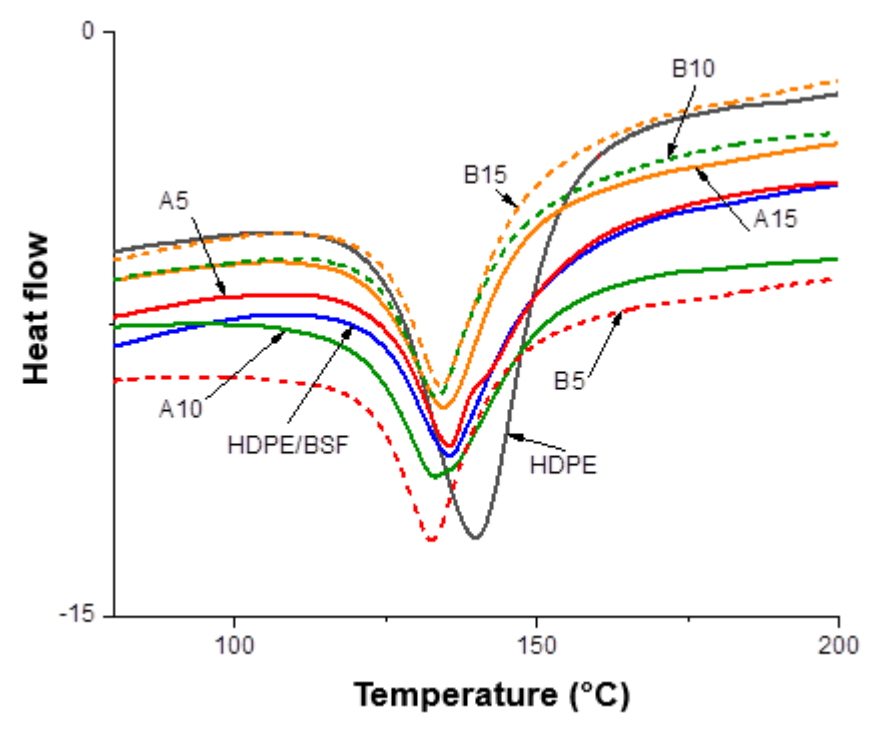


Fig. 10. The DSC thermograms of composites

Table 5. Thermal Properties of the Neat HDPE and HDPE Composites with the BSF as well as Virgin Glass Fibers or Waste Glass Flour

	$T_{\rm m}$ onset	T_{m}	$T_{\rm m}$ end set	$\Delta H_{ m m}$	X _c (%)
A5	121.75	135.48	155.81	106.88	72.96
A10	118.82	133.16	152.91	110.55	75.46
A15	119.32	134.54	148.09	103.24	70.47
B5	119.43	132.46	143.47	107.25	73.21
B10	120.30	133.55	145.89	111.39	76.03
B15	120.65	134.35	148.42	110.69	75.56
HDPE/BSF	120.77	135.55	151.82	100.61	68.68
HDPE	122.47	140.05	153.55	203.89	69.59

The DSC curves exhibited an endothermic peak for all composites (Fig. 10). A comparative analysis of the HDPE-based composites modified by the addition of the waste glass and glass fibers revealed distinct effects on the crystallinity and thermal properties of the composites. The neat HDPE had the highest melting enthalpy ($\Delta H_{\rm m}$) of 203.9 J/g, indicating maximum crystallinity. However, the incorporation of the BSF to the HDPE significantly reduced the enthalpy to 100.6 J/g, indicating a decrease in crystallinity. As for the composites containing waste glass, the melting enthalpy decreases slightly, ranging from 106.9 J/g for the composite A5 to 103.2 J/g for the composite A15. This indicated that the waste glass moderately disturbed the crystallinity while stabilizing the enthalpy

due to its role as a mechanical reinforcement. In contrast, the glass fiber reinforced composites exhibited more pronounced variations in melting enthalpy, ranging from 107.2 J/g for the composite B5 to 110.7 J/g for the composite B15, indicating a greater disruption of the crystallinity.

Analysis of the crystallinity index (X_c) showed that while the neat HDPE had an index of 69.6%. The addition of waste glass lead to a progressive increase in this index, reaching 75.5% for the composite A10, suggesting that waste glass acted as an effective nucleating agent. Similarly, glass fibers also increased the X_c value, with a notably high value of 76.0% for B10, acting as a nucleating agent and promoting crystallization (Iroh and Berry 1996), although this effect was accompanied by greater variability in melting enthalpy. As a result, the addition of BSF, waste glass or glass fiber modified the crystalline structure of the HDPE, reducing the T_m and ΔH_m values while increasing the X_c . Thus, the choice between recycled glass and glass fiber in HDPE composites therefore depends on design priorities: recycled glass offers better thermal stability and a controlled increase in crystallinity, while glass fiber offers higher crystallinity at the expense of the greater disruption of the crystalline structure. These results highlight the importance of selecting the type of reinforcement based on specific thermal performance and crystallinity stability requirements for industrial applications.

CONCLUSIONS

The aim of this study was to utilize two problematic waste streams, namely barley stalks and waste glass, as sources for the design and development of a novel high performance polymer composite.

- 1. It was found that the tensile strength and modulus of the high density polyethylene (HDPE) composites produced by adding barley stalks were significantly improved using the barley straw fiber (BSF)/waste glass hybrid.
- 2. In terms of water absorption, the hybrid use of 15 wt% waste glass powder and BSF in the HDPE noticeably improved the water resistance compared to the HDPE/BSF composites. The water absorption results of the composites revealed that glass giber was more effective in the short time immersion while the waste glass was more effective in the prolonged immersion time.
- 3. The waste glass composites exhibited melting temperatures that decreased as the waste glass content increased, indicating that the crystallinity of the HDPE was increasingly disturbed. The neat HDPE had the highest melting enthalpy and showed the maximum crystallinity. However, the incorporation of the 50 wt% of the BSD into HDPE significantly reduced the melting enthalpy, indicating reduced crystallinity. Similarly, the glass fiber composites showed lower melting temperatures than the neat HDPE. The incorporation of the waste glass into the composites can improve the dimensional stability against water and high humidity.
- 4. When evaluating the water resistance, thermal stability, and strength properties of the composite, it can be said that the use of 15 wt% waste glass and 35 wt% BSF hybrid was the optimum ratio. In addition, the use of a compatibilizing agent such as maleic anhydride grafted polyethylene (MAPE) is also proposed to further enhance the interfacial bonding between HDPE and cellulose-based filler. Thus, by reducing the

amount of micro voids that water can enter at the interface, the water absorption rate can be reduced and higher results can be obtained in the mechanical properties.

ACKNOWLEDGMENTS

The authors express their gratitude to the scientific laboratory "Advanced Composite Materials and Technologies" Plekhanov State University of Economics, Mastalygina Elena Evgenievna and Olkhov Anatoly Alexandrovich.

This project was supported by Ongoing Research Funding program, (ORF-2025-7), King Saud University, Riyadh, Saudi Arabia

Data Availability Statement

Data are available on request from the authors.

Ethical Approval

The authors declared no potential conflicts of interest with respect to the research, authorship, and/or publication of this article.

Declaration of Conflicting Interests

The authors declared no potential conflicts of interest with respect to the research, authorship, and/or publication of this article.

REFERENCES CITED

- Anjumol, K.S., Sumsesh, K.R., Vackova, Hanna, J. M., H., Sabu, T., and Spatenka, P. (2023). "Effect of plasma treatment on the morphology, mechanical, and wetting properties of polyethylene/banana fiber composites," *Biomass Conversion and Biorefinery* 14, 30239-30250. DOI: 10.1007/s13399-023-04884-5
- Arivendan, A., Ramakrishnan, S. K., Chen, X., Zhang, Y.-F., Gao, W., Syamani, F. A., Thangiah, W. J. J., and Siva, I. (2024). "Extraction and characterization of novel Prosopis Juliflora bark and Boehmeria nivea fiber for use as reinforcement in the hybrid composites with the effect of curing temperature, fiber length and weight percentages," *International Journal of Biological Macromolecules* 279, article 135093. DOI: 10.1016/j.ijbiomac.2024.135093
- Aruchamy, K., Karuppusamy, M., Krishnakumar, S., Palanisamy, S., Jayamani, M., Sureshkumar, K., Ali, S. K., and Al-Farraj, S. A. (2025). "Enhancement of mechanical properties of hybrid polymer composites using palmyra palm and coconut sheath fibers: the role of tamarind shell powder," *BioResources* 20(1), 698-724. DOI: 10.15376/biores.20.1.698-724
- Ashori, A., and Nourbakhsh, A. (2008). "A comparative study on mechanical properties and water absorption behavior of fiber-reinforced polypropylene composites prepared by OCC fiber and aspen fiber," *Polymer Composites* 29(5), 574-578. DOI: 10.1002/pc.20582
- Awal, A., Ghosh, S., and Sain, M. (2010). "Thermal properties and spectral characterization of wood pulp reinforced bio-composite fibers," *Journal of Thermal*

- Analysis and Calorimetry 99(2), 695-701. DOI: 10973/99/2/article-p695.xml
- Ayrilmis, N., Kanat, G., Yildiz Avsar, E., Palanisamy, S., and Ashori, A. (2024). "Utilizing waste manhole covers and fiberboard as reinforcing fillers for thermoplastic composites," *Journal of Reinforced Plastics and Composites* 07316844241238507. DOI: 10.1177/07316844241238507
- Bambach, M. R. (2020). "Direct comparison of the structural compression characteristics of natural and synthetic fiber-epoxy composites: Flax, jute, hemp, glass and carbon fibers," *Fibers* 8(10), article 62. DOI: 10.3390/fib8100062
- Chen, J., Teng, Z., and Wu, J. (2017a). "Recycling of waste FRP and corn straw in wood plastic composite," *Polymer Composites* 38(10), 2140-2145. DOI: 10.1002/pc.23789
- Chen, W.-Y., Suzuki, T., and Lackner, M. (2017b). *Handbook of Climate Change Mitigation and Adaptation*, School of Public Policy and Urban Affairs Northeastern University Boston, MA, USA. DOI 10.1007/978-3-319-14409-2
- Chen, X., Yu, J., Zhang, Z., and Lu, C. (2011). "Study on structure and thermal stability properties of cellulose fibers from rice straw," *Carbohydrate Polymers* 85(1), 245-250. DOI: 10.1016/j.carbpol.2011.02.022
- Gopinath, R., Billigraham, P., and Sathishkumar, T. P. (2021). "Investigation of physicochemical, mechanical, and thermal properties of new cellulosic bast fiber extracted from the bark of bauhinia purpurea," *Journal of Natural Fibers* 19(14), 9624-9641. DOI: 10.1080/15440478.2021.1990180
- Gurupranes, S. V, Rajendran, I., Gokulkumar, S., Aravindh, M., Sathish, S., and Elias Uddin, M. (2023). "Preparation, characteristics, and application of biopolymer materials reinforced with lignocellulosic fibers," *International Journal of Polymer Science* 2023(1), article 1738967. DOI: 10.1155/2023/1738967
- Iroh, J. O., and Berry, J. P. (1996). "Mechanical properties of nucleated polypropylene and short glass fiber-polypropylene composites," *European Polymer Journal* 32(12), 1425-1429. DOI: 10.1016/S0014-3057(96)00078-X
- ISO 62 (2008). "Plastics determination of water absorption," International Organization of Standardization, Geneva, Switzerland.
- ISO 178 (2019). "Plastics determination of flexural properties," International Organization of Standardization, Geneva, Switzerland.
- ISO 291 (2008). "Plastics. standard atmospheres for conditioning and testing," International Organization of Standardization, Geneva, Switzerland
- ISO 527-2 (2012). "Plastics determination of tensile properties. Part 2: Test conditions for moulding and extrusion plastics," International Organization of Standardization, Geneva, Switzerland
- Jeziorska, R., Szadkowska, A., Zielecka, M., Wenda, M., and Kepska, B. (2017). "Morphology and thermal properties of HDPE nanocomposites: Effect of spherical silica surface modification and compatibilizer," *Polymer Degradation and Stability* 145, 70-78. DOI: 10.1016/j.polymdegradstab.2017.06.007
- Kar, A., Saikia, D., Palanisamy, S., and Pandiarajan, N. (2024). "Calamus tenuis fiber reinforced epoxy composites: Effect of fiber loading on the tensile, structural, crystalline, thermal and morphological characteristics," Journal of Polymer Research 31(11), 1-16. DOI: 10.1007/s10965-024-04162-6
- Karthik, A., Bhuvaneshwaran, M., Senthil Kumar, M. S., Palanisamy, S., Palaniappan, M., and Ayrilmis, N. (2024). "A review on surface modification of plant fibers for enhancing properties of biocomposites," *ChemistrySelect* 9(21), article e202400650. DOI: 10.1002/slct.202400650

- Kim, S., and Dale, B. E. (2004). "Global potential bioethanol production from wasted crops and crop residues," *Biomass and Bioenergy* 26(4), 361-375. DOI: 10.1016/j.biombioe.2003.08.002
- Kuzmin, A., Ashori, A., Pantyukhov, P., Zhou, Y., Guan, L., and Hu, C. (2024). "Mechanical, thermal, and water absorption properties of HDPE/barley straw composites incorporating waste rubber," *Scientific Reports* 14(1), article 25232. DOI: 10.1038/s41598-024-76337-6
- Kuzmin, A. M., Ayrilmis, N., and Vodyakov, V. N. (2021). "Mechanical properties of barley straw/HDPE composites produced with extrusion process," in: *Defect and Diffusion Forum*, 593-598. DOI: 10.4028/www.scientific.net/DDF.410.593
- Makhlouf, A., Belaadi, A., Amroune, S., Bourchak, M., and Satha, H. (2022). "Elaboration and characterization of flax fiber reinforced high density polyethylene biocomposite: effect of the heating rate on thermo-mechanical properties," *Journal of Natural Fibers* 19(10), 3928-3941. DOI: 10.1080/15440478.2020.1848737
- Mayandi, K., Rajini, N., Ayrilmis, N., Devi, M. P. I., Siengchin, S., Mohammad, F., and Al-Lohedan, H. A. (2020). "An overview of endurance and ageing performance under various environmental conditions of hybrid polymer composites," *Journal of Materials Research and Technology* 9(6), 15962-15988. DOI: 10.1016/j.jmrt.2020.11.031
- Nur Diyana, A. F., Khalina, A., Sapuan, M. S., Lee, C. H., Aisyah, H. A., Nurazzi, M. N., and Ayu, R. S. (2022). "Physical, mechanical, and thermal properties and characterization of natural fiber composites reinforced poly (lactic acid): Miswak (Salvadora persica L.) fibers," International Journal of Polymer Science 2022(1), article 7253136. DOI: 10.1155/2022/7253136
- Pahlevani, F., and Sahajwalla, V. (2018). "Waste glass powder–Innovative value-adding resource for hybrid wood-based products," *Journal of Cleaner Production* 195, 215-225. DOI: 10.1016/j.jclepro.2018.05.205
- Palumbo, M., Formosa, J., and Lacasta, A. M. (2015). "Thermal degradation and fire behaviour of thermal insulation materials based on food crop by-products," *Construction and Building Materials* 79, 34-39. DOI: 10.1016/j.conbuildmat.2015.01.028
- Prasad, L., Kapri, P., Patel, R. V., Yadav, A., and Winczek, J. (2023). "Physical and mechanical behavior of ramie and glass fiber reinforced epoxy resin-based hybrid composites," *Journal of Natural Fibers* 20(2), 1-13. DOI: 10.1080/15440478.2023.2234080
- Puglia, D., Luzi, F., Lilli, M., Sbardella, F., Pauselli, M., Torre, L., and Benincasa, P. (2020). "Straw fibers from barley hybrid lines and their reinforcement effect in polypropylene based composites," *Industrial Crops and Products* 154, article 112736. DOI: 10.1016/j.indcrop.2020.112736
- Ramakrishnan, S. K., Arivendan, A., and Vijayananth, K. (2025). "Cellulose extraction from red sage fiber, Prosopis Juliflora fiber, vegetable waste filler: Applications in PLA based bio composites," *International Journal of Biological Macromolecules* 285, article 138102. DOI: 10.1016/j.ijbiomac.2024.138102

- Ramakrishnan, S. K., Vijayananth, K., Arivendan, A., and Ammarullah, M. I. (2024). "Evaluating the effects of pineapple fiber, potato waste filler, surface treatment, and fiber length on the mechanical properties of polyethylene composites for biomedical applications," *Results in Engineering* 24, article 102974. DOI: 10.1016/j.rineng.2024.102974
- Saleh, M., Al-Hajri, Z., Popelka, A., and Javaid Zaidi, S. (2020). "Preparation and characterization of alumina HDPE composites," *Materials* 13(1), article 250. DOI: 10.3390/ma13010250
- Sanjay, M. R., and Yogesha, B. (2017). "Studies on natural/glass fiber reinforced polymer hybrid composites: An evolution," *Materials Today: Proceedings* 4(2), 2739-2747. DOI: 10.1016/j.matpr.2017.02.151
- Sathish, S., Kumaresan, K., Prabhu, L., and Vigneshkumar, N. (2017). "Experimental investigation on volume fraction of mechanical and physical properties of flax and bamboo fibers reinforced hybrid epoxy composites," *Polymers and Polymer Composites* 25(3), 229-236. DOI: 10.1177/096739111702500309
- Serra-Parareda, F., Julián, F., Espinosa, E., Rodríguez, A., Espinach, F. X., and Vilaseca, F. (2020). "Feasibility of barley straw fibers as reinforcement in fully biobased polyethylene composites: Macro and micro mechanics of the flexural strength," *Molecules* 25(9), article 2242. DOI: 10.3390/molecules25092242
- Suja, R. N., Sridevi, B., and Chitra, M. (2024). "Determination of kinetic parameters and thermal decomposition of epoxy-moringa gum biocomposite using thermogravimetric analysis," *Indian Journal of Chemical Technology (IJCT)* 31(6), 889-901.
- Sumesh, K. R., Ajithram, A., Anjumol, K. S., and Sai Krishnan, G. (2024). "Influence of natural fiber addition and fiber length in determining the wear resistance of epoxybased composites," *Polymer Composites* 45(4), 3029-3042. DOI: 10.1002/pc.27968
- Sumesh, K. R., and Kanthavel, K. (2022). "Optimizing various parameters influencing mechanical properties of banana/coir natural fiber composites using grey relational analysis and artificial neural network models," *Journal of Industrial Textiles* 51(4), 6705S-6727S. DOI: 10.1177/1528083720930304
- Sumesh, K. R., Kavimani, V., Rajeshkumar, G., Indran, S., and Khan, A. (2022). "Mechanical, water absorption and wear characteristics of novel polymeric composites: impact of hybrid natural fibers and oil cake filler addition," *Journal of Industrial Textiles* 51(4S) 5910 S-5937S. DOI: 10.1177/1528083720971344
- TabkhPaz, M., Behravesh, A. H., Shahi, P., and Zolfaghari, A. (2013). "Procedure effect on the physical and mechanical properties of the extruded wood plastic composites," *Polymer Composites* 34(8), 1349-1356. DOI: 10.1002/pc.22549
- Tan, M. Y., Nicholas Kuan, H. T., and Lee, M. C. (2017). "Characterization of alkaline treatment and fiber content on the physical, thermal, and mechanical properties of ground coffee waste/oxobiodegradable HDPE biocomposites," *International Journal of Polymer Science* 2017(1), article 6258151. DOI: 10.1155/2017/6258151
- Then, Y. Y., Ibrahim, N. A., Zainuddin, N., Ariffin, H., and Wan Yunus, W. M. Z. (2013). "Oil palm mesocarp fiber as new lignocellulosic material for fabrication of polymer/fiber biocomposites," *International Journal of Polymer Science* 2013(1), article 797452. DOI: 10.1155/2013/797452
- Zafar, M. J., Elsayed, H., and Bernardo, E. (2024). "Waste glass upcycling supported by alkali activation: An overview," *Materials* 17(9), article 2169. DOI: 10.3390/ma17092169

Zhang, X., Wang, Z., Cong, L., Nie, S., and Li, J. (2020). "Effects of fiber content and size on the mechanical properties of wheat straw/recycled polyethylene composites," *Journal of Polymers and the Environment* 28, 1833-1840. DOI: 10.1007/s10924-020-01733-8

Article submitted: March 24, 2025; Peer review completed: May 28, 2025; Revised version received and accepted: May 31, 2025; Published: June 5, 2025.

DOI: 10.15376/biores.20.3.5967-5987